Prognostic Implications of ^{68}Ga-FAPI-46 PET/CT–Derived Parameters on Overall Survival in Various Types of Solid Tumors

Masao Watanabe[1,2], Wolfgang P. Fendler[1,2], Hong Grafe[1,2], Nader Hirmas[2], Rainer Hamacher[3], Helena Lanzafame[2], Kim M. Pabst[2], Hubertus Hautzel[1], Clemens Aigner[4], Stefan Kasper[3], Bastian von Tresckow[5], Martin Stuschke[6], Sherko Kümmel[7], Celine Lugnier[8], Boris Hadaschik[9], Viktor Grünwald[3,9], Fadi Zarrad[2], Jens T. Siveke[10,11], Ken Herrmann[1,2], and Manuel Weber[1,2]

[1]Department of Nuclear Medicine, University Clinic Essen, Essen, Germany; [2]Department of Nuclear Medicine, University of Duisburg–Essen and German Cancer Consortium–University Hospital Essen, Essen, Germany; [3]Department of Medical Oncology, West German Cancer Center, University of Duisburg–Essen and German Cancer Consortium–University Hospital Essen, Essen, Germany; [4]Department of Thoracic Surgery and Thoracic Endoscopy, University of Duisburg–Essen and German Cancer Consortium–University Hospital Essen, Essen, Germany; [5]Department of Hematology and Stem Cell Transplantation, West German Cancer Center and German Cancer Consortium (DKTK partner site Essen), University Hospital Essen, University of Duisburg–Essen, Essen, Germany; [6]Department of Radiation Therapy, University of Duisburg–Essen and German Cancer Consortium–University Hospital Essen, Essen, Germany; [7]Department of Gynecology and Gynecologic Oncology, Evang. Kliniken Essen–Mitte, Essen, Germany, and Department of Gynecology with Breast Center, Charité–Universitätsmedizin Berlin, Berlin, Germany; [8]Department of Hematology and Oncology with Palliative Care, Ruhr University Bochum, Bochum, Germany; [9]Department of Urology, University of Duisburg–Essen and German Cancer Consortium–University Hospital Essen, Essen, Germany; [10]Bridge Institute of Experimental Tumor Therapy, West German Cancer Center, University Hospital Essen, Essen, Germany; and [11]Division of Solid Tumor Translational Oncology, German Cancer Center Consortium (DKTK partner site Essen), and German Cancer Research Center, Heidelberg, Germany

Tumoral fibroblast activation protein expression is associated with proliferation and angiogenesis and can be visualized by PET/CT. We examined the prognostic value of [^{68}Ga]Ga-fibroblast activation protein inhibitor (FAPI) (^{68}Ga-FAPI)–46 PET/CT for different tumor entities in patients enrolled in 2 prospective imaging studies (NCT05160051, $n = 30$; NCT04571086, $n = 115$). **Methods:** Within 4 wk, 145 patients underwent ^{68}Ga-FAPI-46 and [^{18}F]FDG (^{18}F-FDG) PET/CT. The association between overall survival (OS) and sex, age, tumor entity, total lesion number, highest SUV_{max}, and the presence of each nodal, visceral, and bone metastasis was tested using univariate Cox regression analysis. Multivariate analyses were performed for prognostic factors with P values of less than 0.05. **Results:** In the univariate analysis, shorter OS was associated with total lesion number and the presence of nodal, visceral, and bone metastases on ^{68}Ga-FAPI-46 PET/CT (hazard ratio [HR], 1.06, 2.18, 1.69, and 2.05; $P < 0.01$, < 0.01, $= 0.04$, and $= 0.02$, respectively) and ^{18}F-FDG PET/CT (HR, 1.05, 2.31, 1.76, and 2.30; $P < 0.01$, < 0.01, $= 0.03$, and < 0.01, respectively) and with SUV_{max} on ^{68}Ga-FAPI-46 PET/CT (HR, 1.03; $P = 0.03$). In the multivariate analysis, total lesion number on ^{68}Ga-FAPI-46 PET/CT was an independent risk factor for shorter OS (HR, 1.05; $P = 0.02$). In patients with pancreatic cancer, shorter OS was associated with total lesion number on ^{68}Ga-FAPI-46 PET/CT (HR, 1.09; $P < 0.01$) and bone metastases on ^{18}F-FDG PET/CT (HR, 31.39; $P < 0.01$) in the univariate analysis and with total lesion number on ^{68}Ga-FAPI-46 PET/CT (HR, 1.07; $P = 0.04$) in the multivariate analyses. In breast cancer, total lesion number on ^{68}Ga-FAPI-46 PET/CT (HR, 1.07; $P = 0.02$), as well as bone metastases on ^{18}F-FDG PET/CT (HR, 9.64; $P = 0.04$), was associated with shorter OS in the univariate analysis. The multivariate analysis did not reveal significant prognostic factors. In thoracic cancer (lung cancer and pleural mesothelioma), the univariate and multivariate analyses did not reveal significant prognostic factors. **Conclusion:** Disease extent on ^{68}Ga-FAPI-46 PET/CT is a predictor of short OS and may aid in future risk stratification by playing a supplemental role alongside ^{18}F-FDG PET/CT.

Key Words: ^{68}Ga-FAPI-46; PET/CT; ^{18}F-FDG; overall survival; total lesion number

J Nucl Med 2024; 65:1027–1034
DOI: 10.2967/jnumed.123.266981

In vivo visualization of fibroblast activation protein (FAP) by means of [^{68}Ga]Ga-FAP inhibitor (FAPI) (^{68}Ga-FAPI) PET/CT imaging is characterized by high tumor uptake and low background accumulation of radioligands (*1*). This results in high detection rates in a multitude of solid tumors in comparison with [^{18}F]FDG (^{18}F-FDG) PET/CT (*2–4*).

FAP expression has been confirmed in many cancers (90% of carcinomas), especially in the stroma in the tumor tissue, and thus may become a universal marker of cancer-associated fibroblasts (*5*). This expression has been associated with proliferation, invasion, angiogenesis, and drug resistance (*5*), leading to a poor prognosis in several malignancies, including gastric (*5*), colorectal (*6*), pancreatic (*7*), and non–small cell lung (*8*) cancer. However, only a few studies, mostly on small cohorts, have examined the prognostic value of ^{68}Ga-FAPI PET/CT in this context (*9–11*).

To address this gap in knowledge, we compared the prognostic implications of ^{68}Ga-FAPI-46 PET/CT and ^{18}F-FDG PET/CT in a large population of patients with various tumors.

Received Oct. 31, 2023; revision accepted May 7, 2024.
For correspondence or reprints, contact Masao Watanabe (d7he4ng@gmail.com).
Published online May 23, 2024.
COPYRIGHT © 2024 by the Society of Nuclear Medicine and Molecular Imaging.

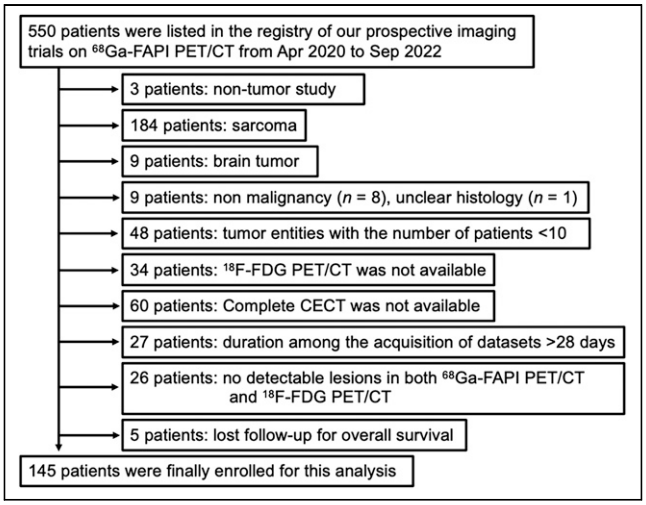

FIGURE 1. Consolidated Standards of Reporting Trials (CONSORT) diagram illustrating enrollment process. CECT = contrast-enhanced CT.

MATERIALS AND METHODS

Patients

We screened our institutional database of prospective imaging studies for consecutive patients who underwent ^{68}Ga-FAPI-46 PET/CT and ^{18}F-FDG PET/CT within 4 wk from April 2020 to September 2022 for imaging of tumors other than sarcoma (because of another ongoing project focused on sarcoma). The patient selection process is shown in Figure 1.

All patients gave written informed consent. Of these, 145 patients were included in 2 prospective imaging studies (NCT05160051, 30 interventional; NCT04571086, 115 observational). Data analysis was approved by the ethics committee of the University of Duisburg–Essen (20-9485-BO and 19-8991-BO). The patient subgroups have previously been reported (*12–16*). We obtained the precursor of ^{68}Ga-FAPI-46 from SOFIE Biosciences.

Image Acquisition

At 23.3 ± 20.2 min (range, 9–102 min) after the injection of 123.9 ± 31.0 MBq (range, 60–199 MBq) of ^{68}Ga-FAPI-46, PET/CT was performed on a Siemens 128-slice Biograph mCT (26/145 patients, 17.9%), Siemens Biograph Vision (115/145 patients, 79.3%), or Philips Vereos (4/145 patients, 2.8%). Acquisition times were based on a prior publication by our group (*13*).

^{18}F-FDG PET/CT was performed 71.8 ± 18.2 min (range, 43–147 min) after the injection of 267.1 ± 84.6 MBq (range, 94–458 MBq) of ^{18}F-FDG. Images were acquired on a Biograph mCT (27/145 patients, 18.6%), Biograph Vision (109/145 patients, 75.2%), or Vereos (9/145 patients, 6.2%). All PET images were iteratively reconstructed with time of flight (Biograph mCT: 3 iterations and 21 subsets, gaussian filtering of 4 mm; Biograph Vision: 4 iterations and 5 subsets, gaussian filtering of 2 mm; Vereos: 2 iterations and 10 subsets, gaussian filtering of 4 mm).

Image Interpretation and Quantitative Analysis

Images were interpreted by a board-certified nuclear medicine physician and radiologist with 14 y of experience, who had completed institutional reader training on 50 ^{68}Ga-FAPI-46 PET/CT datasets including common pitfalls. The reader was not aware of the clinical information. Masked interpretation was chosen to avoid biases due to knowledge of clinical information and to measure the standalone impact of the imaging modalities, even though lack of clinical information may trigger faulty image interpretation at times.

Lesions were classified as malignant if they exhibited focal tracer accumulation incongruent with physiologic or nonneoplastic uptake (*17*) and were categorized into the following anatomic regions: primary, cervicothoracic nodal metastases, abdominopelvic nodal metastases, pulmonary metastases, hepatic metastases, other visceral metastases, and bone metastases. Lesion number (≤10 per region to avoid individual bias, from larger to smaller lesions), and SUV_{max} was assessed visually on Syngo.via software (Siemens Healthineers). Representative diagnosis cases are shown in Figures 2 and 3.

Statistical Analysis

Overall survival (OS) was defined as the interval from the day of the PET/CT scans (^{68}Ga-FAPI-46 PET/CT and ^{18}F-FDG PET/CT) until death or the end of the study (censored in June 2023). For OS, we performed univariate Cox proportional hazards regression analysis using the following variables: sex, age, restaging (vs. initial staging), tumor entity, total lesion number, the presence of nodal metastases, the presence of visceral metastases, the presence of bone metastases, and the highest SUV_{max} of all lesions. Prognostic factors with a P value of less than 0.05 in the univariate analysis, as well as the tumor entity as a categoric parameter (considering the heterogeneity of tumor characteristics), were considered statistically significant and tested in multivariate analyses. We also performed subanalyses for the patients with pancreatic cancer, breast cancer, and thoracic cancer (lung cancer and pleural mesothelioma). Separate Cox analyses for each tumor entity (pancreatic cancer, breast cancer, and thoracic cancer) are susceptible to multiple-comparison problems due to small sample sizes. To resolve this issue, we entered into the multivariate Cox analysis only the prognostic parameters that were significant predictors of OS in the multivariate analysis on the entire cohort. We performed Kaplan–Meier analysis using log-rank testing to determine the statistical association between OS and findings on ^{18}F-FDG PET/CT and ^{68}Ga-FAPI-46 PET/CT. For statistical analysis, we used MedCalc version 22.007, 32-bit (MedCalc Software), and Prism 8 (GraphPad Software). Numeric values are provided as mean ± SD.

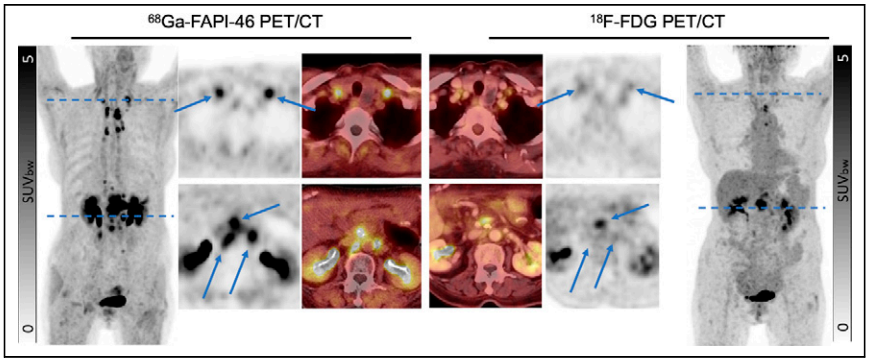

FIGURE 2. Intraindividual comparison between ^{68}Ga-FAPI-46 PET/CT and ^{18}F-FDG PET/CT for restaging in patient with postoperative pancreatic head cancer (73-y-old woman with extensive nodal metastases). Bilateral nodal metastases in supraclavicular region were detectable only on ^{68}Ga-FAPI-46 PET/CT (SUV_{max}, 5.74 on right side and 10.19 on left side; arrows); findings on ^{18}F-FDG PET/CT were nonspecific (SUV_{max}, 2.93 on right side and 3.58 on left side; arrows). At level of bilateral renal pelvis, there were 3 and only 1 detectable paraaortic nodal metastases on ^{68}Ga-FAPI-46 PET/CT (SUV_{max}, 6.75, 11.37, and 11.75 from right to left) and ^{18}F-FDG PET/CT (SUV_{max}, 7.94; other 2 lymph nodes not measurable), respectively (arrows). SUV_{bw} = SUV based on body weight.

RESULTS

Patient Cohort

The final cohort included 145 patients, of whom 85 were male and 60 were female (mean ± SD, 61.6 ± 11.8 y old; range, 30–85 y old). We enrolled 53 patients (36.6%) for staging and 92 patients (63.4%) for restaging. The most common tumor entities were pancreatic cancer (n = 40), mesothelioma (pleural, n = 18; peritoneal, n = 2), and breast cancer (n = 17). Sixty-four of 145 (44.1%) patients died during the mean follow-up period of 13.8 mo (range, 1–30 mo). Patient characteristics are provided in Table 1. Because we enrolled patients requiring either staging or restaging, we classified only the patients with T(positive)/N0/M0, T(any)/N(positive)/M0, and T(any)/N(any)/M(positive), by referring to the ^{68}Ga-FAPI-46 PET/CT, ^{18}F-FDG PET/CT, and contrast-enhanced CT, all of which were performed within 4 wk. The median total lesion number was 4 on ^{68}Ga-FAPI-46 PET/CT (range, 0–53; 1 with no lesions; 44 with 1 lesion; 27 with 2 or 3 lesions; 8 with 4 or 5 lesions; 20 with 6–10 lesions; 45 with >10 lesions) and 3 on ^{18}F-FDG PET/CT (range, 0–57; 8 with no lesions; 47 with 1 lesion; 26 with 2 or 3 lesions; 7 with 4 or 5 lesions; 20 with 6–10 lesions; 37 with >10 lesions).

The treatment records were available for 133 of 145 patients (91.7%). Ninety-four of 145 patients (64.8%) underwent surgery. In 93 cases (93/145, 64.1%), the primary was resected, and in 22 cases (22/145, 15.2%), metastases were resected; in 21 of those, both the primary and metastases were resected (21/145, 14.5%).

Of the 94 patients who underwent surgery, 79 (79/145, 54.5%) received systemic therapy (chemotherapy or immunotherapy). Of the remaining 39 recorded patients without surgery (39/145, 26.9%), 31 (31/145, 21.4%) received systemic therapy. Systemic therapy was used in 110 of 145 (75.9%) patients, of whom 14 had breast cancer, 5 had lung cancer, 14 had pleural mesothelioma, 2 had peritoneal mesothelioma, 13 had cholangiocellular cancer, 33 had pancreatic cancer, 13 had colorectal cancer, 9 had renal cell cancer, and 7 had

TABLE 1
Patient Characteristics (n = 145)

Clinical variable	Value
Mean age (y)	61.6 (range, 30–85)
Male/female	85 (58.6%)/60 (41.4%)
Staging/restaging	53 (36.6%)/92 (63.4%)
Primary tumor	
Breast cancer	17 (11.7%)
T+N0M0/T(any)N+M0/T(any)N(any)M1	5 (3.4%)/4 (2.8%)/8 (5.5%)
Lung cancer	12 (8.3%)
T+N0M0/T(any)N+M0/T(any)N(any)M1	6 (4.1%)/1 (0.7%)/5 (3.4%)
Mesothelioma (pleural/peritoneal)	18 (12.4%)/2 (1.4%)
T+N0M0/T(any)N+M0/T(any)N(any)M1	6 (4.1%)/7 (4.8%)/7 (4.8%)
Cholangiocellular cancer	15 (10.3%)
T+N0M0/T(any)N+M0/T(any)N(any)M1	3 (2.1%)/2 (1.4%)/10 (6.9%)
Pancreatic cancer	40 (27.6%)
T+N0M0/T(any)N+M0/T(any)N(any)M1	11 (7.6%)/7 (4.8%)/22 (15.2%)
Colorectal cancer	15 (10.3%)
T+N0M0/T(any)N+M0/T(any)N(any)M1	3 (2.1%)/0 (0%)/12 (8.3%)
Renal cell cancer	15 (10.3%)
T+N0M0/T(any)N+M0/T(any)N(any)M1	5 (3.4%)/1 (0.7%)/9 (6.2%)
Prostate cancer	11 (7.6%)
T+N0M0/T(any)N+M0/T(any)N(any)M1	4 (2.8%)/0 (0%)/7 (4.8%)
Treatment data, available/not available	133 (91.7%)/12 (8.3%)
Surgery for primary site/metastases	93 (64.1%)/22 (15.2%)
Chemo- or immunotherapy, surgical cases	79 (54.5%)
Neoadjuvant/adjuvant/salvage/unspecified	21 (14.5%)/46 (31.7%)/53 (36.6%)/5 (3.4%)
Chemo- or immunotherapy, no surgery	31 (21.4%)
Other therapy	
RPT/radioembolization/^{223}Ra	4 (2.8%)/3 (2.1%)/1 (0.7%)
Hormone/RFA/radiation therapy	11 (7.6%)/2 (1.4%)/38 (26.2%)

RPT = radiopharmaceutical therapy; RFA = radiofrequency ablation.
Values are number and percentage, except for age.

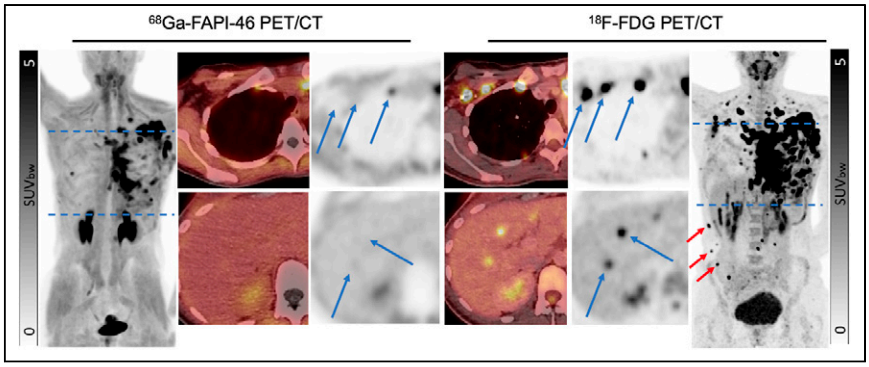

FIGURE 3. Intraindividual comparison between ^{68}Ga-FAPI-46 PET/CT and ^{18}F-FDG PET/CT for restaging in patient with postoperative left breast cancer (36-y-old woman with large number of metastases). Several metastases to muscles were detectable only on ^{18}F-FDG PET/CT (red arrows). At same axillary level (right side of body), there were 1 and 3 detectable nodal metastases on ^{68}Ga-FAPI-46 PET/CT (SUV_{max}, 3.47; other 2 distal lymph nodes not measurable) and on ^{18}F-FDG PET/CT (SUV_{max}, 26.28, 18.54, and 29.60 from proximal to distal lymph nodes), respectively (blue arrows). In liver region (lower part of images), 2 liver metastases were detectable on ^{18}F-FDG PET/CT (SUV_{max}, 6.65 in segment 4 and 4.50 in segment 5); however, no liver metastases were detectable on ^{68}Ga-FAPI-46 PET/CT (blue arrows). SUV_{bw} = SUV based on body weight.

prostate cancer. Other therapies consisted of radiopharmaceutical therapy with [^{177}Lu]Lu-PSMA-617 (n = 4), radioembolization (n = 3), [^{223}Ra]Ra-chloride (n = 1), hormone therapy (for breast cancer and prostate cancer, n = 11), radiofrequency ablation (n = 2), and external-beam radiotherapy (n = 38). Information on the treatment is summarized in Table 1.

Prognostic Analysis

In the univariate analysis for ^{68}Ga-FAPI-46 PET/CT, total lesion number; the presence of nodal, visceral, and bone metastases; and the highest SUV_{max} of all lesions were significant predictors of short OS (hazard ratio [HR], 1.06, 2.18, 1.69, 2.05, and 1.03, respectively; 95% CI, 1.03–1.08, 1.32–3.60, 1.03–2.77, 1.12–3.77, and 1.00–1.07, respectively; $P < 0.01$, < 0.01, $= 0.04$, $= 0.02$, and $= 0.03$, respectively; Table 2). In the multivariate analysis (Table 2), total lesion number was significantly associated with OS (HR, 1.05; 95% CI, 1.01–1.10; $P = 0.02$), whereas the presence of nodal, visceral, and bone metastases and the highest SUV_{max} of all lesions were not (HR, 1.12, 1.10, 2.21, and 1.02, respectively; 95% CI, 0.57–2.19, 0.56–2.16, 0.93–5.26, and 0.98–1.07, respectively; $P = 0.75$, 0.78, 0.07, and 0.29, respectively). Kaplan–Meier curves for OS based on the total lesion number are shown in Figure 4 using the median total lesion number (n = 4) as the cutoff. The median survival of patients with at least 4 lesions (73 patients) versus less than 4 lesions (72 patients) was 17 and 25 mo, respectively ($P < 0.001$).

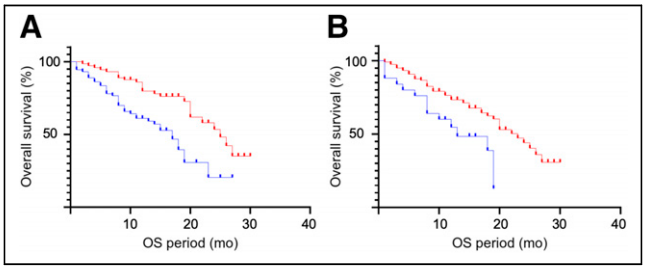

FIGURE 4. Kaplan–Meier analyses for OS regarding total lesion number on ^{68}Ga-FAPI-46 PET/CT (A) and presence of bone metastases on ^{18}F-FDG PET/CT (B). Blue and red lines are groups with ≥4 total lesions (median value of all patients) and those with ≤3 total lesions in A ($P <$ 0.001) and group with positive bone metastases and those with negative bone metastases in B ($P < 0.005$), respectively.

Regarding ^{18}F-FDG PET/CT (Table 2), total lesion number and the presence of nodal, visceral, and bone metastases were significantly associated with shorter OS (HR, 1.05, 2.31, 1.76, and 2.30, respectively; 95% CI, 1.03–1.08, 1.41–3.80, 1.07–2.92, and 1.27–4.17, respectively; $P < 0.01$, < 0.01, $= 0.03$, and < 0.01, respectively). In the multivariate analysis (Table 2), the presence of bone metastases was a predictor of shorter OS (HR, 3.46; 95% CI, 1.49–8.03; $P < 0.01$), whereas total lesion number and the presence of nodal and visceral metastases were not (HR, 1.04, 1.53, and 1.20, respectively; 95% CI, 0.999–1.08, 0.81–2.88, and 0.60–2.39, respectively; $P = 0.055$, 0.19, and 0.61, respectively). Kaplan–Meier curves for OS in the group with positive bone metastases (25 patients) and those with negative bone metastases (120 patients) are shown in Figure 4. The median survival was 13 and 23 mo, respectively ($P < 0.005$).

Regarding ^{68}Ga-FAPI-46 PET/CT in the patients with pancreatic cancer, total lesion number was significantly associated with shorter OS in the univariate analysis (HR, 1.09; 95% CI, 1.03–1.15; $P < 0.01$) and in the multivariate analysis (HR, 1.07; 95% CI, 1.004–1.13; $P = 0.04$). For ^{18}F-FDG PET/CT, bone metastases were a significant prognostic indicator for shorter OS in the univariate analysis (HR, 31.39; 95% CI, 4.33–227.36; $P < 0.01$). In the multivariate analysis, bone metastases were borderline-significant (HR, 8.67; 95% CI, 0.91–82.78; $P = 0.06$). These results are summarized in Table 3.

As for the patients with breast cancer using ^{68}Ga-FAPI-46 PET/CT, total lesion number was significantly associated with shorter OS in the univariate analysis (HR, 1.07; 95% CI, 1.01–1.13; $P = 0.02$) but was not significant in the multivariate analysis (HR, 1.03; 95% CI, 0.95–1.11; $P = 0.47$). For ^{18}F-FDG PET/CT, bone metastases were a significant prognostic indicator for OS in the univariate analysis (HR, 9.64; 95% CI, 1.12–83.30; $P = 0.04$) but was not significant in the multivariate analysis (HR, 5.58; 95% CI, 0.38–81.50; $P = 0.21$). These results are summarized in Table 4.

Concerning the subanalysis for patients with thoracic cancer, including lung cancer and pleural mesothelioma, no PET-derived prognostic factors were not associated with OS in the uni- and multivariate analyses. These results are summarized in Table 5.

DISCUSSION

The results of our study reveal that ^{68}Ga-FAPI-46 PET/CT–based parameters have prognostic value in a mixed population of cancer patients. The presence of bone metastases on ^{18}F-FDG PET/CT, and lesion number on ^{68}Ga-FAPI-46 PET/CT (HR, 1.05), were independent risk factors for shorter OS in the multivariate analysis. Although the HR of the latter may appear small, continuous variables with a wide range (0–53) often display lower

TABLE 2
Uni- and Multivariate Analyses of OS Using Cox Proportional Hazards Regression Analysis
(Death Events, $n = 64$; Censored, $n = 81$)

	Univariate		Multivariate	
Parameter	HR	*P*	HR	*P*
^{68}Ga-FAPI-46 PET/CT				
Sex	1.25 (0.75–2.08)	0.40		
Age	1.01 (0.99–1.03)	0.31		
Restaging vs. initial staging	1.70 (0.98–2.93)	0.06		
Tumor entity*				
Mesothelioma ($n = 20$)	0.77 (0.37–1.59)	0.48	0.62 (0.28–1.34)	0.22
Breast cancer ($n = 17$)	0.67 (0.27–1.64)	0.38	0.30 (0.10–0.90)	0.03
Cholangiocarcinoma ($n = 15$)	0.56 (0.23–1.36)	0.20	0.43 (0.17–1.06)	0.07
Renal cell carcinoma ($n = 15$)	0.33 (0.10–1.10)	0.07	0.22 (0.06–0.84)	0.03
Colorectal cancer ($n = 15$)	0.44 (0.15–1.26)	0.13	0.39 (0.13–1.18)	0.10
Lung cancer ($n = 12$)	0.27 (0.06–1.14)	0.08	0.19 (0.04–0.85)	0.03
Prostate cancer ($n = 11$)	0.53 (0.20–1.38)	0.19	0.27 (0.08–0.91)	0.03
Total lesion number	1.06 (1.03–1.08)	<0.01	1.05 (1.01–1.10)	0.02
Nodal metastases	2.18 (1.32–3.60)	<0.01	1.12 (0.57–2.19)	0.75
Visceral metastases	1.69 (1.03–2.77)	0.04	1.10 (0.56–2.16)	0.78
Bone metastases	2.05 (1.12–3.77)	0.02	2.21 (0.93–5.26)	0.07
Highest SUV_{max}	1.03 (1.00–1.07)	0.03	1.02 (0.98–1.07)	0.29
^{18}F-FDG PET/CT				
Tumor entity*				
Mesothelioma ($n = 20$)	0.77 (0.37–1.59)	0.48	0.50 (0.23–1.06)	0.07
Breast cancer ($n = 17$)	0.67 (0.27–1.64)	0.38	0.20 (0.06–0.62)	<0.01
Cholangiocarcinoma ($n = 15$)	0.56 (0.23–1.36)	0.20	0.39 (0.16–0.97)	0.04
Renal cell carcinoma ($n = 15$)	0.33 (0.10–1.10)	0.07	0.16 (0.04–0.60)	<0.01
Colorectal cancer ($n = 15$)	0.44 (0.15–1.26)	0.13	0.30 (0.10–0.92)	0.03
Lung cancer ($n = 12$)	0.27 (0.06–1.14)	0.08	0.17 (0.04–0.75)	0.02
Prostate cancer ($n = 11$)	0.53 (0.20–1.38)	0.19	0.20 (0.06–0.69)	0.01
Total lesion number	1.05 (1.03–1.08)	<0.01	1.04 (0.999–1.08)	0.055
Nodal metastases	2.31 (1.41–3.80)	<0.01	1.53 (0.81–2.88)	0.19
Visceral metastases	1.76 (1.07–2.92)	0.03	1.20 (0.60–2.39)	0.61
Bone metastases	2.30 (1.27–4.17)	<0.01	3.46 (1.49–8.03)	<0.01
Highest SUV_{max}	1.02 (0.995–1.05)	0.11		

*Compared with pancreatic cancer.
Data are mean followed by 95% CI in parentheses.

HRs. Yet the effect of lesion number on the extreme ends of the spectrum is not negligible, as shown in the context of Ki-67, an established prognostic parameter in a multitude of malignancies, where HRs in the similar range are commonly observed (e.g., 1.05 in patients with adrenocortical carcinoma regarding OS (*18*)). In addition, the univariate analysis identified metastases to nodes, visceral organs, and bone and the highest SUV_{max} of all lesions on ^{68}Ga-FAPI-46 PET/CT as significant prognostic indicators for shorter OS. ^{68}Ga-FAPI-46 PET/CT–based parameters such as total lesion number, and ^{18}F-FDG PET/CT–based parameters such as the presence of hypermetabolic bone metastases, may aide risk stratification alongside other, already-established, prognostic markers (*19*). ^{18}F-FDG PET/CT as a prognostic marker is well established in a multitude of malignancies, underpinned by an extensive body of research, and is well understood, especially with regard to its associations with dedifferentiation and proliferation. ^{18}F-FDG PET/CT–derived markers that have been well studied in their association with OS are, among others, metabolic tumor volume and total lesion glycolysis, such as in patients with lung, pancreatic, and breast cancer (*19–21*).

On the basis of our results, it appears unlikely that ^{68}Ga-FAPI-46 PET/CT–derived markers will generally replace ^{18}F-FDG PET/CT,

TABLE 3
Uni- and Multivariate Subanalyses of OS for Patients with Pancreatic Cancer Using Cox Proportional Hazards Regression Analysis (Death Events, $n = 28$; Censored, $n = 12$)

	Univariate		Multivariate	
Parameter	HR	*P*	HR	*P*
^{68}Ga-FAPI-46 PET/CT				
Total lesion number	1.09 (1.03–1.15)	<0.01	1.07 (1.004–1.13)	0.04
^{18}F-FDG PET/CT				
Bone metastases	31.39 (4.33–227.36)	<0.01	8.67 (0.91–82.78)	0.06

Data are mean followed by 95% CI in parentheses.

yet they may serve as complementary markers, with lesion number being particularly promising. The latter may be the consequence of a better diagnostic performance in some tumor entities (*2*,*4*,*11*). Additionally, the identification of PET biomarkers derived from ^{68}Ga-FAPI-46 PET/CT can be of particular interest in tumor entities, where it could eventually become the gold standard for PET imaging (*22*).

^{68}Ga-FAPI-46 PET/CT may therefore aid treatment decisions not just by providing accurate staging but also by providing prognostic information. The impact on patient prognosis has previously been shown in the context of patients with colorectal cancer, where FAP expression on ^{68}Ga-FAPI-46 PET/CT was associated with a significantly shorter relapse-free survival (*9*).

In our subanalysis of patients with pancreatic cancer, bone metastases (HR, 31.39; 95% CI, 4.33–227.36; $P < 0.01$) in ^{18}F-FDG PET/CT were significantly associated with shorter OS in the univariate analysis and showed borderline significance (HR, 8.67; 95% CI, 0.91–82.78; $P = 0.06$) in the multivariate analysis. On the other hand, with regard to ^{68}Ga-FAPI-46 PET/CT–derived parameters, only total lesion number reached statistical significance in the univariate analysis (HR, 1.09; 95% CI, 1.03–1.15; $P < 0.01$) and multivariate analysis (HR, 1.07; 95% CI, 1.004–1.13; $P = 0.04$).

A prior study on pancreatic cancer has shown that SUV_{max} in ^{68}Ga-FAPI-04 PET/CT had a significant independent prognostic value for recurrence-free survival and that total pancreatic FAP expression (the sum of the multiplication of SUV_{mean} and total FAPI-avid volume) was a significant prognostic indicator for OS (*10*). Similarly, in a published metaanalysis, tumor SUV_{max} on ^{18}F-FDG PET/CT has been shown to be a significant prognostic factor for OS (*19*). Furthermore, a high glycolytic activity in pancreatic cancer has been linked with subtypes that commonly exhibit a poor prognosis (e.g., basal subtype) and is associated with metastatic spread (*23*). In our study, we additionally found that total lesion number on ^{68}Ga-FAPI-46 PET/CT could be a useful prognostic factor for OS in patients with pancreatic cancer. Importantly, the presence of bone metastases on PET/CT correlated more strongly with OS for ^{18}F-FDG than for ^{68}Ga-FAPI-46 in our study. This may be partly attributable to the fact that of the 4 of 39 patients with bone metastases secondary to pancreatic cancer, bone metastases were detected by ^{18}F-FDG PET/CT, by ^{68}Ga-FAPI-46 PET/CT, and by both modalities in 2, 3, and 1 cases, respectively. The large discrepancy in HR between the 2 modalities may therefore be caused by the low number of positive cases in the subgroup with pancreatic cancer.

To our knowledge, this was the first study to report on the prognostic implications of FAPI PET/CT in patients with breast cancer:

In our cohort, total lesion number on ^{68}Ga-FAPI-46 PET/CT, and bone metastases on ^{18}F-FDG PET/CT, were significant prognostic indicators for shorter OS in the univariate analysis; however, total lesion number on ^{68}Ga-FAPI-46 PET/CT and bone metastases on ^{18}F-FDG PET/CT were not significant in the

TABLE 4
Uni- and Multivariate Subanalyses of OS for Patients with Breast Cancer Using Cox Proportional Hazards Regression Analysis (Death Events, $n = 6$; Censored, $n = 11$)

	Univariate		Multivariate	
Parameter	HR	*P*	HR	*P*
^{68}Ga-FAPI-46 PET/CT				
Total lesion number	1.07 (1.01–1.13)	0.02	1.03 (0.95–1.11)	0.47
^{18}F-FDG PET/CT				
Bone metastases	9.64 (1.12–83.30)	0.04	5.58 (0.38–81.50)	0.21

Data are mean followed by 95% CI in parentheses.

TABLE 5
Uni- and Multivariate Subanalyses of OS for Patients with Thoracic Cancer Using Cox Proportional Hazards Regression Analysis (Death Events, $n = 11$; Censored, $n = 19$)

	Univariate	
Parameter	HR	*P*
^{68}Ga-FAPI-46 PET/CT		
Total lesion number	1.01 (0.93–1.10)	0.78
^{18}F-FDG PET/CT		
Bone metastases	1.62 (0.20–13.01)	0.65

Data are mean followed by 95% CI in parentheses.

multivariate analysis. The prognostic value of ^{18}F-FDG PET/CT has been shown by an expansive body of evidence, for which a correlation between glycolytic activity on the one hand and tumor aggressiveness and poor prognosis on the other hand could be established (*20*,*24*). The lack of statistically significant results in the multivariate analysis may at least partially be attributable to insufficient statistical power due to the sample size.

A central limitation of this study is the low number of patients for each tumor entity, potentially affecting statistical power and calling for further prospective analyses on larger cohorts. Especially for the Cox subanalysis, there are few total events and few events per variable (*25*). Also, it has yet to be determined which PET-derived parameters can most accurately predict OS. Future multicenter prospective analyses with a larger sample size may be warranted to confirm the results. In addition, the 50 cases used to train the reader may be a limitation, since interobserver agreement has been shown to be moderate at this experience level; an experience level of at least 300 cases may be needed for substantial agreement (*26*). The prognostic parameters we assessed could complement risk stratification alongside already-established risk factors, such as resection status and neural invasion in the context of pancreatic cancer (*27*,*28*). Also, the absence of segmentation of PET-derived whole-body tumor volume and whole-body SUV_{mean} may be a major limitation.

CONCLUSION

Here, we demonstrate an association of disease extent (parametrized by total lesion number on ^{68}Ga-FAPI-46 PET/CT) on the one hand and OS on the other hand in various malignancies, such as pancreatic cancer. In line with prior publications, ^{18}F-FDG PET/CT allowed for stratification of prognosis, especially in the presence of bone metastases. Improved risk stratification may aid patient management in the future.

DISCLOSURE

Masao Watanabe obtained a postdoctoral fellowship from Humboldt Foundation. Wolfgang Fendler reports fees from SOFIE Biosciences (research funding), Janssen (consultant, speaker), Calyx (consultant, image review), Bayer (consultant, speaker, research funding), Novartis (speaker, consultant), Telix (speaker), GE Healthcare (speaker), Eczacıbaşı Monrol (speaker), Abx (speaker), Amgen (speaker), and Urotrials (speaker), outside the submitted work. Rainer Hamacher reports grants from the Clinician Science Program of the University Medicine Essen Clinician Scientist Academy. He also reports other support from Eli Lilly and Company, Novartis, and PharmaMar, as well as personal fees from PharmaMar and Eli Lilly and Company, outside the submitted work. Kim Pabst reports personal fees and research funds from Bayer Healthcare, outside the submitted work, as well as a Junior Clinician Scientist Stipend from the University Medicine Essen Clinician Scientist Academy and travel fees from IPSEN. Stefan Kasper received honoraria from Merck Serono, MSD, Novartis, BMS, Amgen, Roche, Sanofi-Aventis, Servier, Incyte, Pierre Fabre, and Lilly and research funding from Lilly, BMS, and Roche. Bastian von Tresckow is an advisor or consultant for Allogene, Amgen, BMS/Celgene, Cerus, Gilead Kite, Incyte, IQVIA, Lilly, Merck Sharp & Dohme, Miltenyi, Novartis, Noscendo, Pentixapharm, Pfizer, Pierre Fabre, Qualworld, Roche, Sobi, and Takeda; has received honoraria from AbbVie, AstraZeneca, BMS/Celgene, Gilead Kite, Incyte, Lilly, Merck Sharp & Dohme, Novartis, Roche Pharma AG, and Takeda; reports research funding from Esteve (to the institution), Merck Sharp & Dohme (to the institution), Novartis (to the institution), and Takeda (to the institution); and reports travel support from AbbVie, AstraZeneca, Gilead Kite, Lilly, Merck Sharp & Dohme, Pierre Fabre, Roche, Takeda, and Novartis, all outside the submitted work. Sherko Kümmel reports a consultant or advisory role with Roche/Genentech, Genomic Health, Novartis, AstraZeneca, Amgen, Celgene, SOMATEX, Daiichi Sankyo, pfm medical, Pfizer, MSD Oncology, Lilly, Sonoscape, Gilead Sciences, Seagen, and Agendia. He also reports travel support and expenses from Roche, Daiichi Sankyo, and Gilead Sciences and an uncompensated relationship with WSG. Boris Hadaschik declares grants to the institution from Novartis, BMS, and the German Research Foundation; consulting fees from ABX, Accord, Amgen, AstraZeneca, Bayer, BMS, Janssen, Lightpoint Medical, and Pfizer; payment for lectures from Accord, Astellas, Janssen, and Monrol; support for travel or attending meetings from Bayer, Ipsen, and Janssen; and participation on data safety monitoring boards for Janssen, all outside the submitted work. Viktor Grünwald has received honoraria from Bristol-Myers Squibb, Pfizer, Ipsen, Eisai, MSD Oncology, Merck HealthCare, EUSAPharm, Apogepha, and Ono Pharmaceutical; has an advisory role with Bristol-Myers Squibb, Pfizer, MSD Oncology, Merck HealthCare, Ipsen, Eisai, Debiopharm, PCI Biotech, Cureteq, and Oncorena; and receives travel funds from Pfizer, Ipsen, and Merck HealthCare. Jens Siveke reports honoraria from AstraZeneca, Bayer, Immunocore, Novartis, Roche/Genentech, and Servier, outside the submitted work. Work in his laboratory is supported by the German Cancer Consortium. His institution receives research funding from Bristol-Myers Squibb, Celgene, Eisbach, Bio, and Roch/Genentech. He holds ownership in and serves on the board of directors of Pharma15. Ken Herrmann reports personal fees from Bayer, SIRTEX, Adacap, Curium, Endocyte, IPSEN, Siemens Healthineers, GE Healthcare, Amgen, Novartis, ymabs, Aktis Oncology, Theragnostics, and Pharma 15; personal fees and other fees from SOFIE Biosciences; nonfinancial support from ABX; and grants and personal fees from BTG, outside the submitted work. Manuel Weber reports personal fees from Boston Scientific, Terumo, Advanced Accelerator Applications, IPSEN, and Eli Lilly, outside the submitted work. No other potential conflict of interest relevant to this article was reported.

KEY POINTS

QUESTION: Do findings from ^{68}Ga-FAPI-46 PET/CT have prognostic implications regarding OS?

PERTINENT FINDINGS: Disease extent derived from ^{68}Ga-FAPI-46 PET/CT is a predictor of OS and may enhance risk stratification in various solid tumors.

IMPLICATIONS FOR PATIENT CARE: Improved tumor detection and risk stratification may aide clinical decisions and the pursuit of personalized medicine.

REFERENCES

1. Meyer C, Dahlbom M, Lindner T, et al. Radiation dosimetry and biodistribution of ^{68}Ga-FAPI-46 PET imaging in cancer patients. *J Nucl Med.* 2020;61:1171–1177.
2. Lan L, Zhang S, Xu T, et al. Prospective comparison of ^{68}Ga-FAPI versus ^{18}F-FDG PET/CT for tumor staging in biliary tract cancers. *Radiology.* 2022;304:648–657.
3. Wang L, Tang G, Hu K, et al. Comparison of ^{68}Ga-FAPI and ^{18}F-FDG PET/CT in the evaluation of advanced lung cancer. *Radiology.* 2022;303:191–199.
4. Pang Y, Zhao L, Luo Z, et al. Comparison of ^{68}Ga-FAPI and ^{18}F-FDG uptake in gastric, duodenal, and colorectal cancers. *Radiology.* 2021;298:393–402.
5. Fitzgerald AA, Weiner LM. The role of fibroblast activation protein in health and malignancy. *Cancer Metastasis Rev.* 2020;39:783–803.
6. Wikberg ML, Edin S, Lundberg IV, et al. High intratumoral expression of fibroblast activation protein (FAP) in colon cancer is associated with poorer patient prognosis. *Tumour Biol.* 2013;34:1013–1020.
7. Cohen SJ, Alpaugh RK, Palazzo I, et al. Fibroblast activation protein and its relationship to clinical outcome in pancreatic adenocarcinoma. *Pancreas.* 2008;37:154–158.
8. Moreno-Ruiz P, Corvigno S, Grootenhuis NCT, et al. Stromal FAP is an independent poor prognosis marker in non-small cell lung adenocarcinoma and associated with p53 mutation. *Lung Cancer.* 2021;155:10–19.
9. Strating E, Wassenaar E, Verhagen M, et al. Fibroblast activation protein identifies consensus molecular subtype 4 in colorectal cancer and allows its detection by ^{68}Ga-FAPI-PET imaging. *Br J Cancer.* 2022;127:145–155.
10. Ding J, Qiu J, Hao Z, et al. Prognostic value of preoperative [^{68}Ga]Ga-FAPI-04 PET/CT in patients with resectable pancreatic ductal adenocarcinoma in correlation with immunohistological characteristics. *Eur J Nucl Med Mol Imaging.* 2023;50:1780–1791.
11. Liu Q, Shi S, Liu S, et al. The added value of [^{68}Ga]Ga-DOTA-FAPI-04 PET/CT in pancreatic cancer: a comparison to [^{18}F]F-FDG. *Eur Radiol.* 2023;33:5007–5016.
12. Kessler L, Ferdinandus J, Hirmas N, et al. ^{68}Ga-FAPI as a diagnostic tool in sarcoma: data from the ^{68}Ga-FAPI PET prospective observational trial. *J Nucl Med.* 2022;63:89–95.
13. Ferdinandus J, Kessler L, Hirmas N, et al. Equivalent tumor detection for early and late FAPI-46 PET acquisition. *Eur J Nucl Med Mol Imaging.* 2021;48:3221–3227.
14. Kessler L, Ferdinandus J, Hirmas N, et al. Pitfalls and common findings in ^{68}Ga-FAPI PET: a pictorial analysis. *J Nucl Med.* 2022;63:890–896.
15. Hirmas N, Hamacher R, Sraieb M, et al. Fibroblast activation protein positron emission tomography and histopathology in a single-center database of 324 patients and 21 tumor entities. *J Nucl Med.* 2023;64:711–716.
16. Pabst KM, Trajkovic-Arsic M, Cheung PFY, et al. Superior tumor detection for ^{68}Ga-FAPI-46 versus ^{18}F-FDG PET/CT and conventional CT in patients with cholangiocarcinoma. *J Nucl Med.* 2023;64:1049–1055.
17. Lan L, Liu H, Wang Y, et al. The potential utility of [^{68}Ga]Ga-DOTA-FAPI-04 as a novel broad-spectrum oncologic and non-oncologic imaging agent: comparison with [^{18}F]FDG. *Eur J Nucl Med Mol Imaging.* 2022;49:963–979.
18. Beuschlein F, Weigel J, Saeger W, et al. Major prognostic role of Ki-67 in localized adrenocortical carcinoma after complete resection. *J Clin Endocrinol Metab.* 2015;100:841–849.
19. Zhu D, Wang L, Zhang H, et al. Prognostic value of ^{18}F-FDG-PET/CT parameters in patients with pancreatic carcinoma: a systematic review and meta-analysis. *Medicine (Baltimore).* 2017;96:e7813.
20. Paydary K, Seraj SM, Zadeh MZ, et al. The evolving role of FDG-PET/CT in the diagnosis, staging and treatment of breast cancer. *Mol Imaging Biol.* 2019;21:1–10.
21. Liu J, Dong M, Sun X, Li W, Xing L, Yu J. Prognostic value of ^{18}F-FDG PET/CT in surgical non-small cell lung cancer: a meta-analysis. *PLoS One.* 2016;11:e0146195.
22. Calais J, Mona CE. Will FAPI PET/CT replace FDG PET/CT in the next decade? Point—an important diagnostic, phenotypic, and biomarker role. *AJR.* 2021;216:305–306.
23. Martens S, Lefesvre P, Nicolle R, et al. Different shades of pancreatic ductal adenocarcinoma, different paths towards precision therapeutic applications. *Ann Oncol.* 2019;30:1428–1436.
24. Groheux D, Cochet A, Humbert O, et al. ^{18}F-FDG PET/CT for staging and restaging of breast cancer. *J Nucl Med.* 2016;57(suppl 1):17S–26S.
25. Vittinghoff E, McCulloch CE. Relaxing the rule of ten events per variable in logistic and Cox regression. *Am J Epidemiol.* 2007;165:710–718.
26. Mei R, Kessler L, Pabst KM, et al. ^{68}Ga-FAPI PET/CT interobserver agreement on tumor assessment: an international multicenter prospective study. *J Nucl Med.* 2023;64:1043–1048.
27. Strobel O, Neoptolemos J, Jäger D, Büchler MW. Optimizing the outcomes of pancreatic cancer surgery. *Nat Rev Clin Oncol.* 2019;16:11–26.
28. Iwasaki T, Hiraoka N, Ino Y, et al. Reduction of intrapancreatic neural density in cancer tissue predicts poorer outcome in pancreatic ductal carcinoma. *Cancer Sci.* 2019;110:1491–1502.